Supporting Information

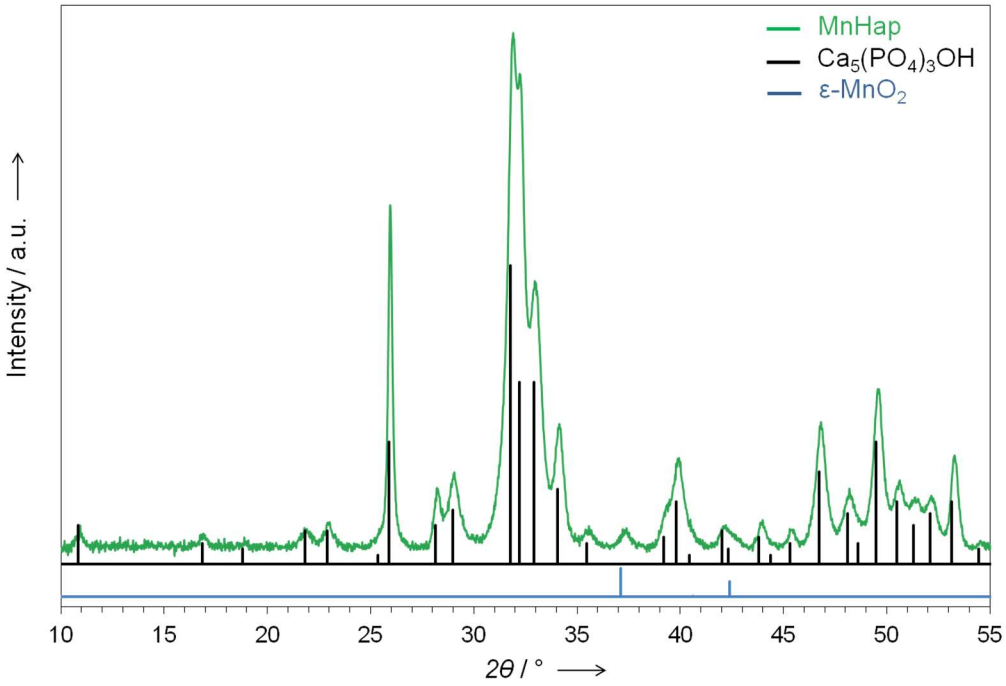

Figure S1. X-ray diffractogram of MnHap solid.

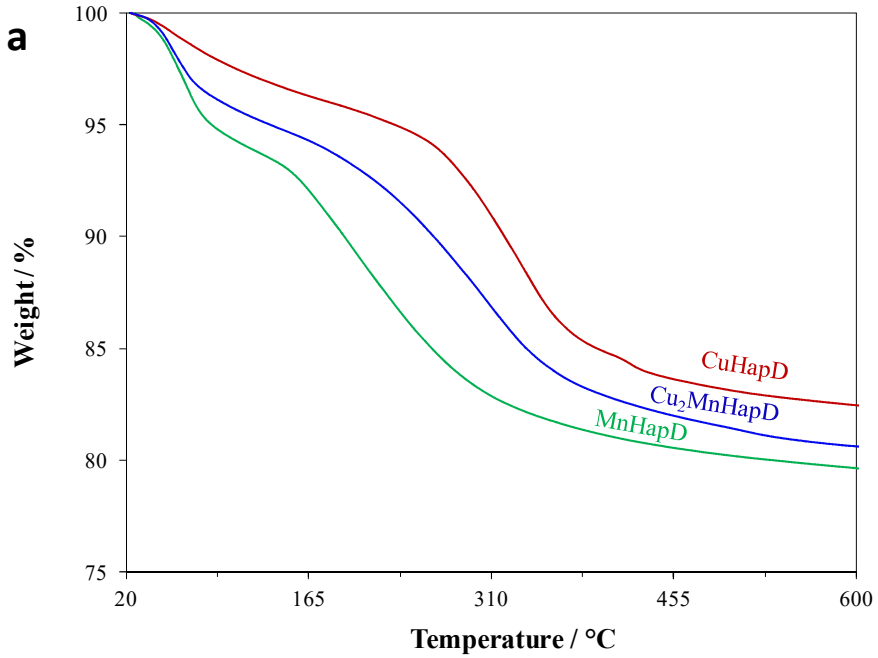

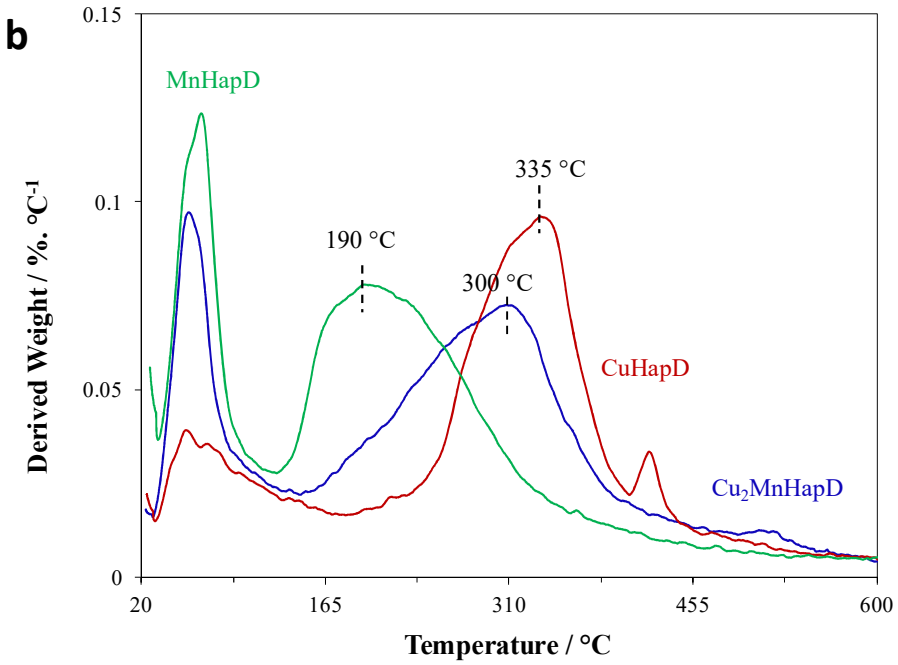

Figure S2. TGA (a) and DTG (b) curves of CuHapD, Cu_2MnHapD and MnHapD samples.

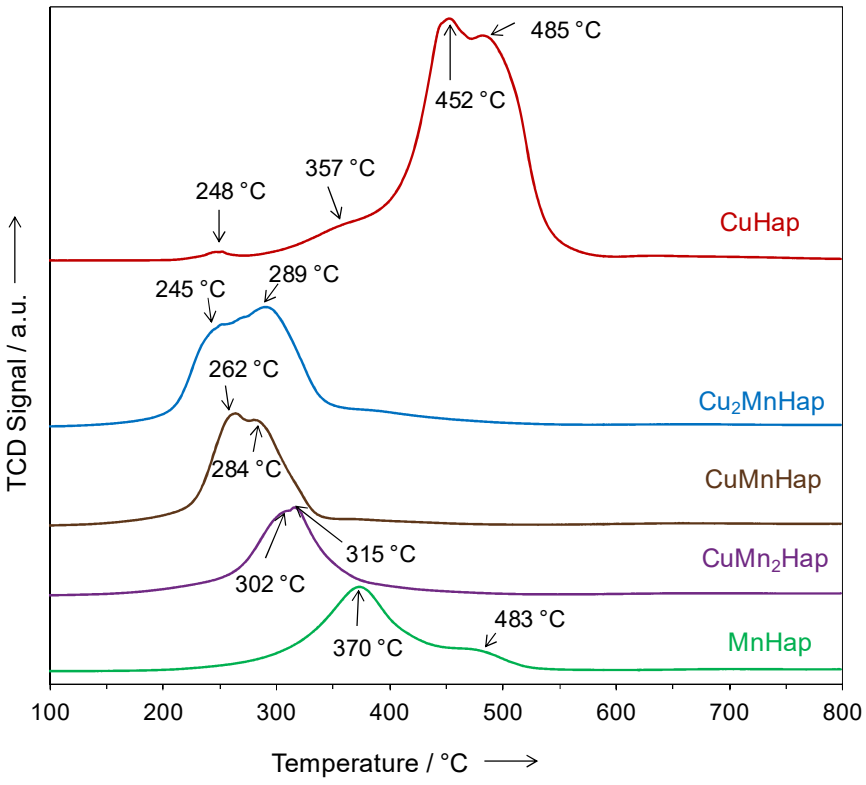

Figure S3. H_2-TPR profiles of Cu_xMn_yHap solids calcined at 400 °C.

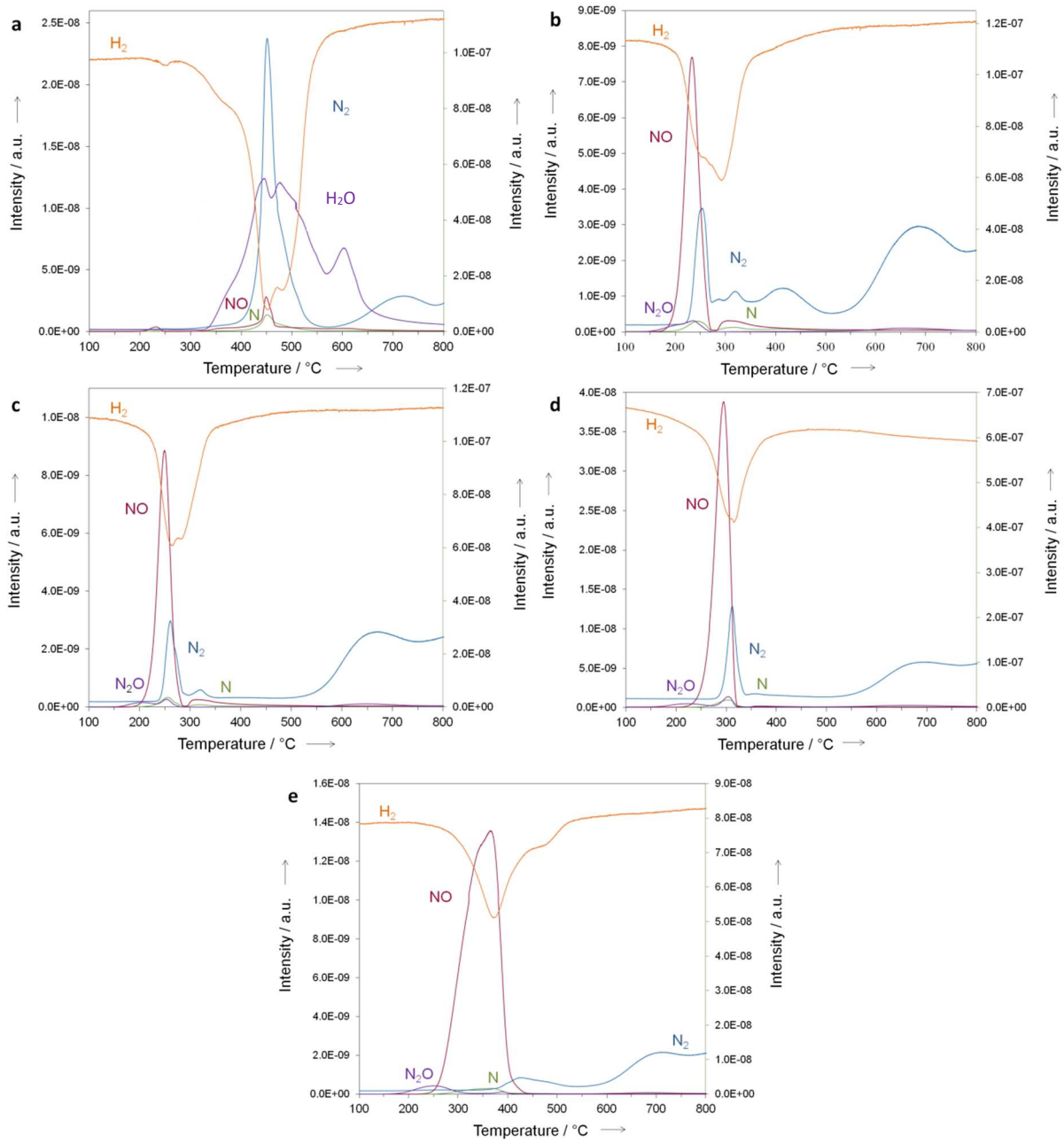

Figure S4. Evolution of the intensity of the signals corresponding to m/z = 2, 14, 17, 28, 30 and 44 as a function of temperature for the solids: a-CuHap; b-Cu_2MnHap; c-CuMnHap; d-$CuMn_2Hap$; e-MnHap. The y-axis on the left gives the intensities of the signals m/z = 14, 17, 28, 30 and 44. The y-axis on the right gives the intensity of the peak m/z = 2.

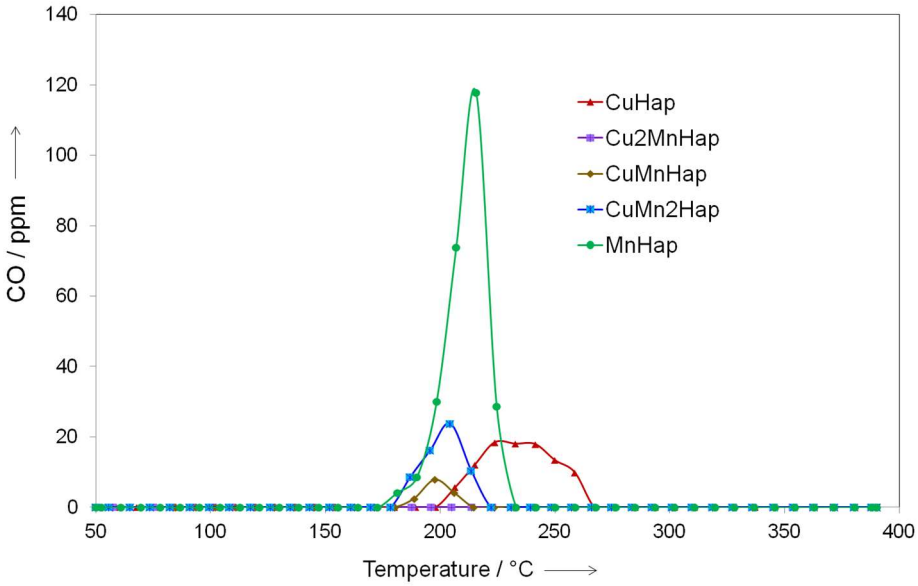

Figure S5. CO production as a function of temperature over Cu_xMn_yHap catalysts.

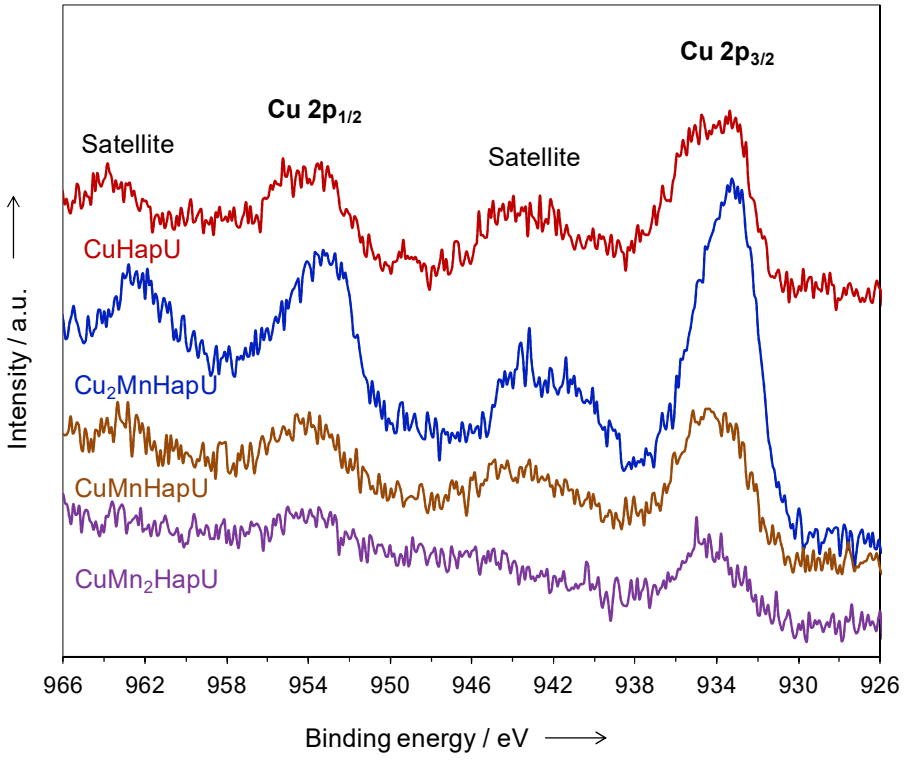

Figure S6. 1st recording of Cu 2p for Cu_xMn_yHapU samples.

Table S1. TGA based data obtained for dried CuHap D, Cu_2MnHap D and MnHap D samples.

Sample	Global weight loss	Experimental weight loss (%)			Theoretical weight loss (%)
		1st step	2nd step	3d step	Nitrates

CuHapD	17.5	4.0 (20 - 180 °C)	11.2 (180 - 400 °C)	2.3 (400 - 600 °C)	13.7
Cu_2MnHapD	19.4	5.1 (20 - 140 °C)	12.0 (140 - 400 °C)	2.3 (400 - 600 °C)	13.6
MnHapD	20.4	6.4 (20 - 130 °C)	12.5 (130 - 400 °C)	1.5 (400 - 600 °C)	13.2

Table S2. XPS based data obtained for fresh and used catalysts.

Sample	Cu $2p_{3/2}$[a]	FWHM Cu $2p_{3/2}$ [a]	I_{sat}/I_{pp}[a]	ΔE
CuHap	932.7	2.69	0.35	0.1
Cu_2MnHap	933.4	326	0.49	0.5
CuMnHap	933.1	3.14	0.49	0.9
$CuMn_2$Hap	933.4	2.78	0.56	1
CuHapU	933.3	3.45	0.29	0
Cu_2MnHapU	933.3	3.07	0.32	0.4
CuMnHapU	933.3	3.20	0.38	0.9
$CuMn_2$HapU	933.4	3.58	0.49	1

[a] Data obtained for 2nd recording.

Table S3. List of ToF-SIMS positive ion fragments detected in copper containing solids

$Cu_xCa_vO_zH_w^+$	$Cu_xP_tO_zH_w^+$	$Cu_xCa_vP_tO_zH_w^+$	$Cu_xO_zH_w^+$
CuCaO	n.d.[a]	Cu_2CaPO_4	Cu ; ^{65}Cu
^{65}CuCaO		$^{65}CuCuCaPO_4$	Cu_2 ; $^{65}CuCu$; $^{65}Cu_2$
$CuCaO_2$		$^{65}Cu_2CaPO_4$	Cu_3 ; $^{65}CuCu_2$;
$CuCaO_2H$			Cu_2O ; $^{65}CuCuO$; $^{65}Cu_2O$
$CuCaO_3$			Cu_3O ; $^{65}CuCu_2O$; $^{65}Cu_2CuO$
$CuCa_3O_4$			Cu_3O_2 ; $^{65}CuCu_2O_2$
$CuCa_2O_3H$			Cu_4O_2 ; $^{65}CuCu_3O_2$; $^{65}Cu_2Cu_2O_2$
$CuCa_3O_4H$			Cu_5O_2 ; $^{65}CuCu_4O_2$; $^{65}Cu_2Cu_3O_2$; $^{65}Cu_3Cu_3O_2$
Cu_2CaO_2H			Cu_5O_3 ; $^{65}CuCu_4O_3$; $^{65}Cu_2Cu_3O_3$
$^{65}CuCuCaO_2H$			Cu_6O_3 ; $^{65}CuCu_5O_3$; $^{65}Cu_2Cu_4O_3$; $^{65}Cu_3Cu_3O_3$
$^{65}Cu_2CaO_2H$			Cu_2OH ; $^{65}CuCuOH$; $^{65}Cu_2OH$
			Cu_3O_2H

[a] Not detected.

Table S4. List of ToF-SIMS positive ion fragments detected in manganese containing solids

$Mn_yCa_vO_zH_w^+$	$Mn_yP_tO_zH_w^+$	$Mn_yCa_vP_tO_zH_w^+$	$Mn_yO_zH_w^+$
MnCaO	$MnPO_2$	Mn_2CaPO_5	Mn
$MnCaO_2$		Mn_2CaPO_4H	Mn_2
Mn_2CaO_2			MnO
Mn_2CaO_3			Mn_2O
Mn_3CaO_4			Mn_2O_2
$MnCa_2O_2$			Mn_2O_4
$MnCa_2O_3$			Mn_2O_5
$Mn_2Ca_2O_4$			Mn_3O_2
$MnCaO_2H$			Mn_3O_3
Mn_2CaO_3H			Mn_2O_2H
$MnCa_2O_3H$			$Mn_2O_2H_2$
			Mn_3O_3H

Table S5. T_{10}, T_{50} and T_{90} (CO_2) obtained in toluene oxidation for Hap and Cu_xMn_yHap catalysts.

Sample	T_{10} (CO_2) [°C]	T_{50} (CO_2) [°C]	T_{90} (CO_2) [°C]
Hap	297	-	-
CuHap	223	255	302
Cu_2MnHap	180	196	213
CuMnHap	180	202	216
$CuMn_2Hap$	185	205	218
MnHap	192	210	224